National Aeronautics and Space Administration

Phased Array Measurements of a Full-Scale Helicopter

Kyle A. Pascioni, Colin M. Stutz, Mary L. Houston

NASA Langley Research Center

James H. Stephenson

U.S. Army Combat Capabilities Development Command

Vertical Flight Society's 81st Annual Forum & Technology Display
Virginia Beach, VA
21 May 2025

Motivation and objective

Motivation

- Acoustic measurements of full-scale, full-aircraft are difficult to interpret
- Signal complexity increases with propulsor count
- Recent progress made to separate harmonic noise per propulsor [2,3]
- Need solution to separate nondeterministic noise per propulsor → source ranking

Objective

- Assess feasibility of rotational beamforming [4] for nondeterministic noise source separation (and quantification)

UH-1A helicopter example spectrum [1]

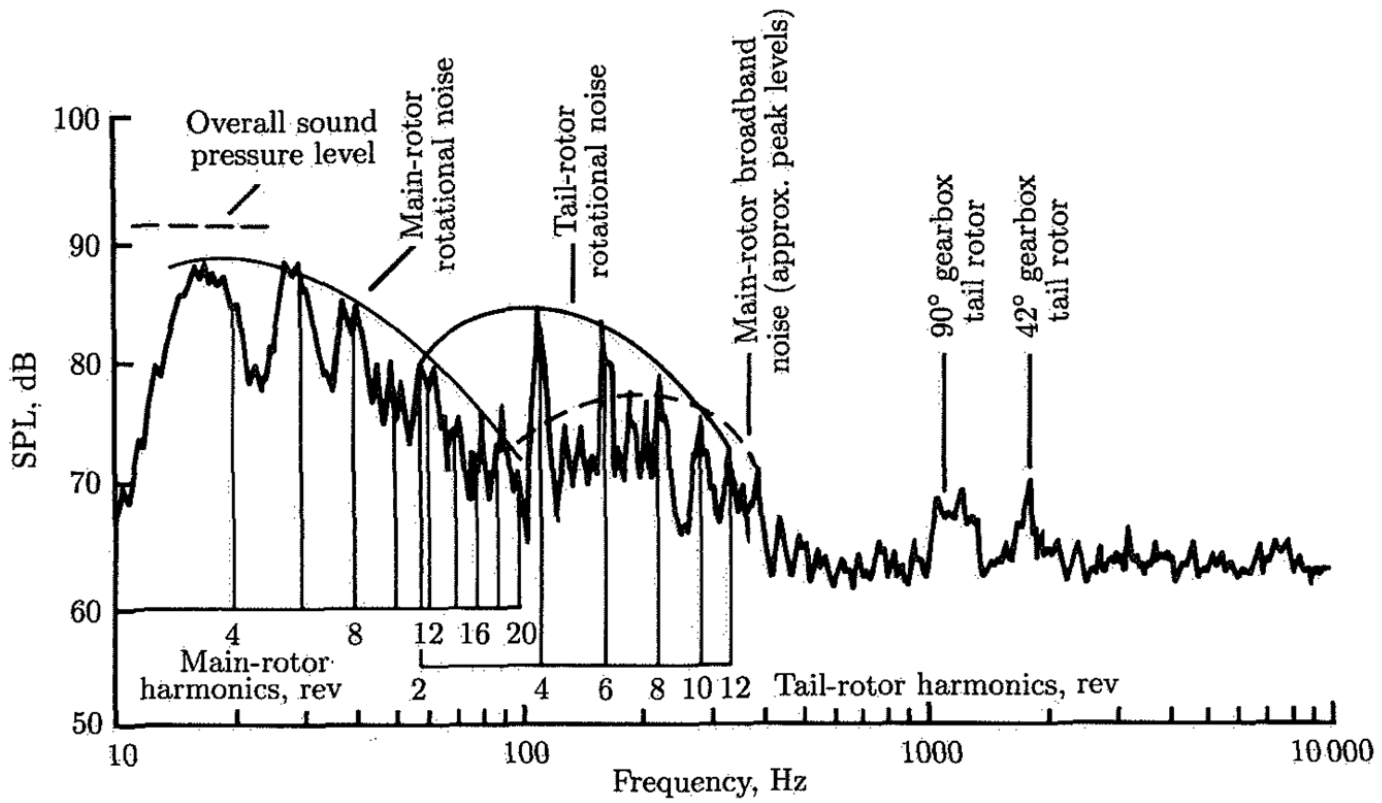

[1]Hubbard , NASA RP 1258, 1991.
[2]Rachaprolu & Greenwood, JAHS, 69(1), 2017.
[3]Pascioni, Thai, & Bain, AIAA 2024-3231.
[4]Sijtsma, Oerlemans, & Holthusen, AIAA 2001-2167.

Motivation and objective

Motivation

- Acoustic measurements of full-scale, full-aircraft are difficult to interpret
- Signal complexity increases with propulsor count
- Recent progress made to separate harmonic noise per propulsor [2,3]
- Need solution to separate nondeterministic noise per propulsor → source ranking

Objective

- Assess feasibility of rotational beamforming [4] for nondeterministic noise source separation (and quantification)

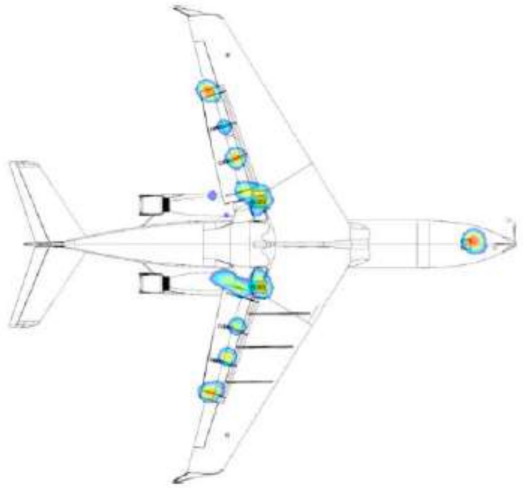

Airframe noise - acoustic flight test
Humphreys et al., NASA TM 2023.

Rotating source beamforming – wind tunnel
Source: Sijtsma, Oerlemans, & Holthusen, AIAA 2001-2167
used with permission

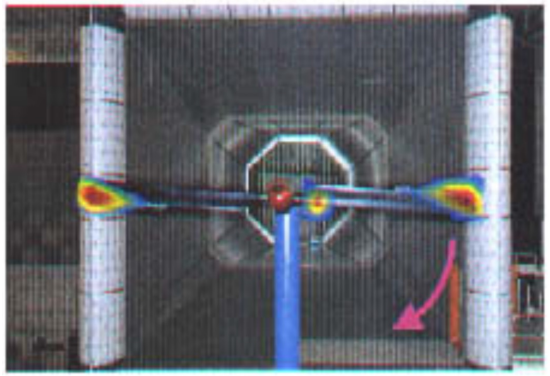

[1]Hubbard , NASA RP 1258, 1991.
[2]Rachaprolu & Greenwood, JAHS, 69(1), 2017.
[3]Pascioni, Thai, & Bain, AIAA 2024-3231.
[4]Sijtsma, Oerlemans, & Holthusen, AIAA 2001-2167.

Test aircraft

MD530F Helicopter

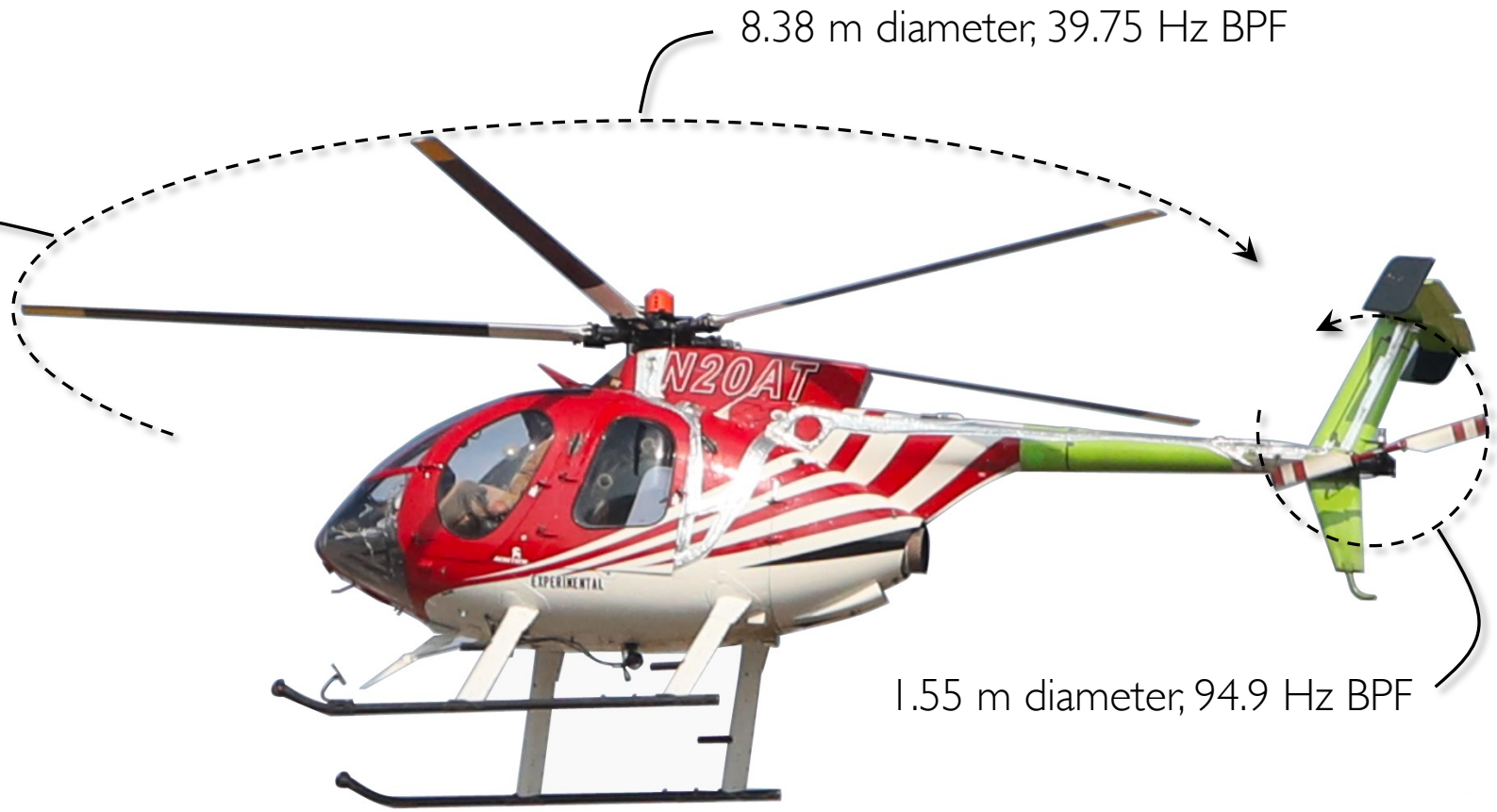

Flight Conditions

20 kt level forward flight

- 60 m AGL
- 30 m AGL

Phased array design

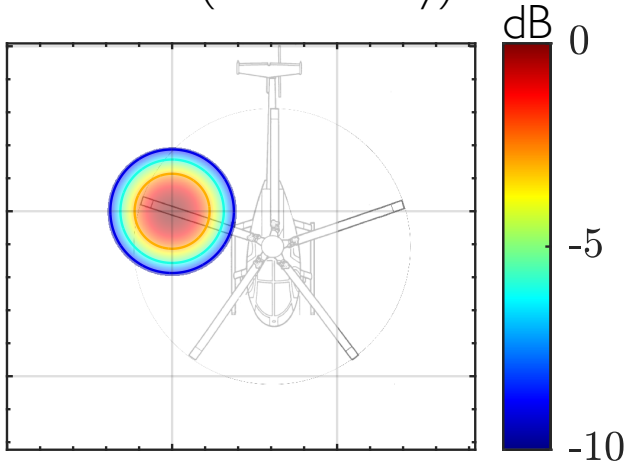

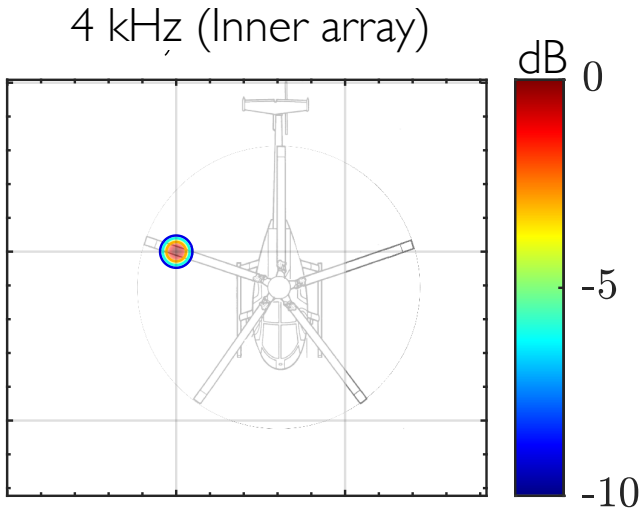

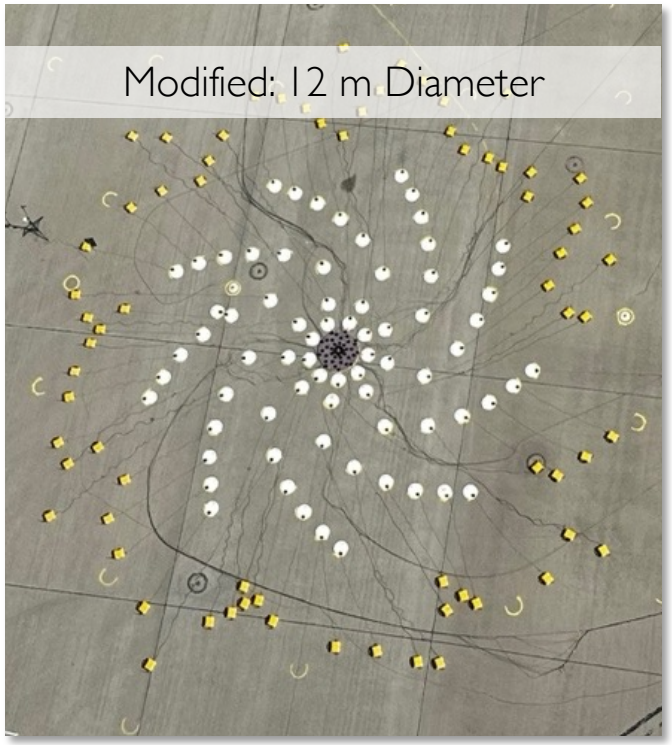

Phased array layout

Array features:

- 117-channel nested array; 72-channel outer, 45 inner
- Each subarray designed to minimize beamwidth while maintaining sidelobe levels 10 dB down [1]
- Combination of GRAS 67AX and Knowles
- Two synchronized DAQs via GPS-based timing

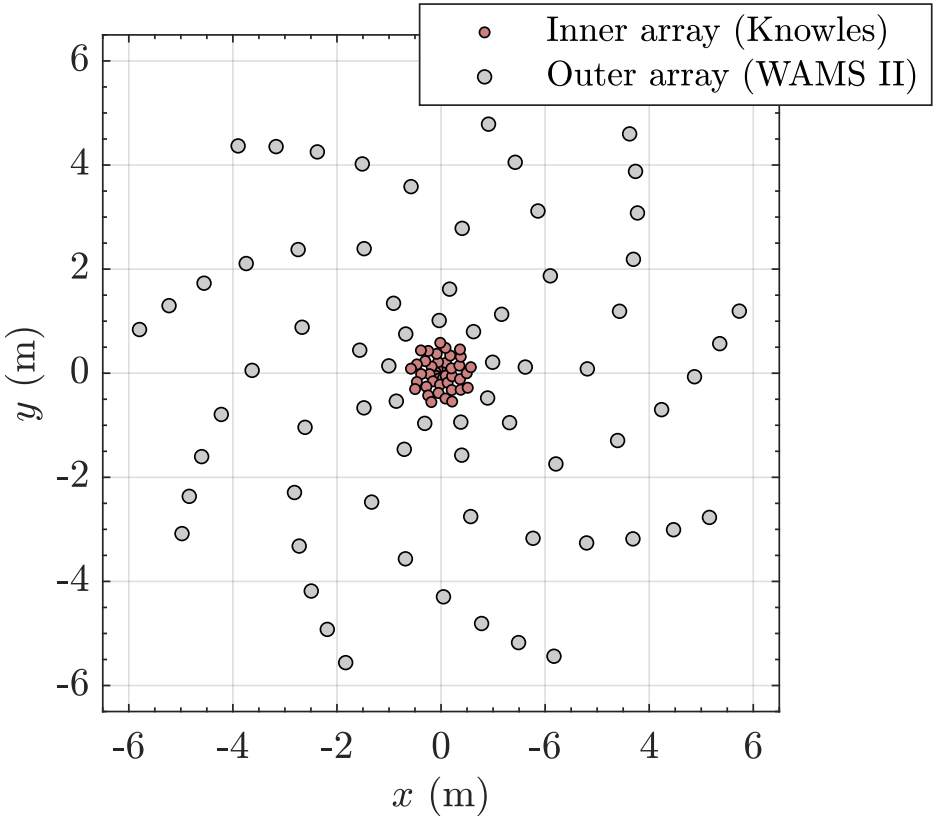

[1]Underbrink, MS Thesis, 1995.

Phased array layout

Array features:

- 117-channel nested array; 72-channel outer, 45 inner
- Each subarray designed to minimize beamwidth while maintaining sidelobe levels 10 dB down [1]
- Combination of GRAS 67AX and Knowles
- Two synchronized DAQs via GPS-based timing

Point spread functions (60 m altitude)

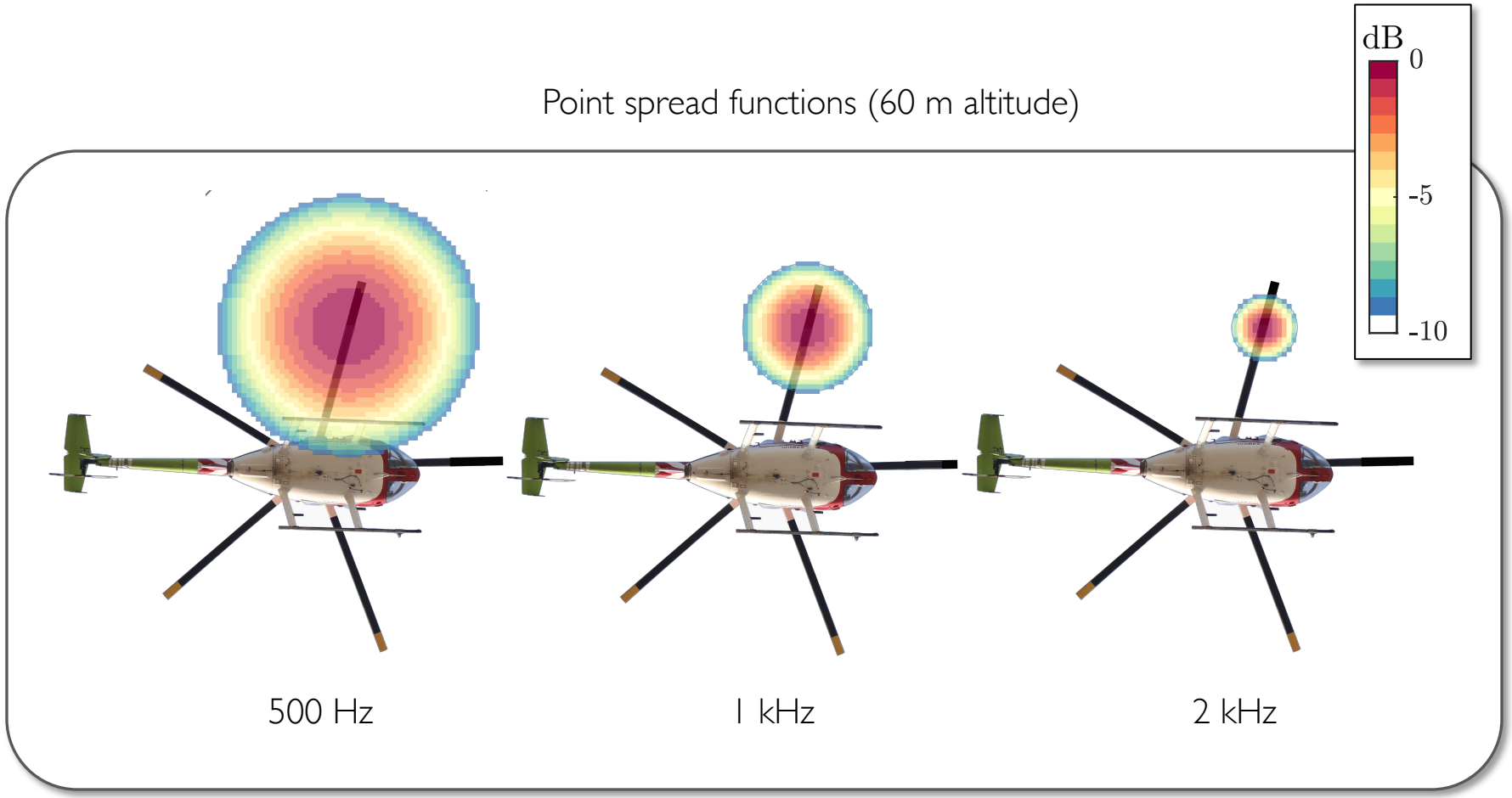

[1]Underbrink, MS Thesis, 1995.

ROtating Source Identifier (ROSI)

- Scan grid translates to follow main rotor hub, and rotates at measured rotation rate, Ω

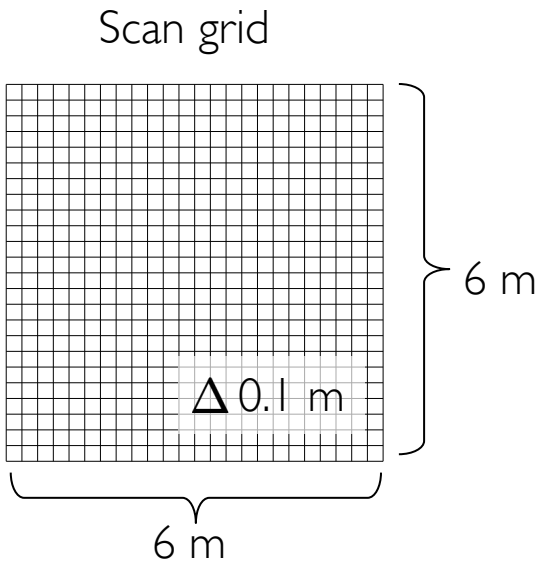

ROtating Source Identifier (ROSI)

- Scan grid **translates** to follow main rotor hub, and **rotates** at measured rotation rate, Ω

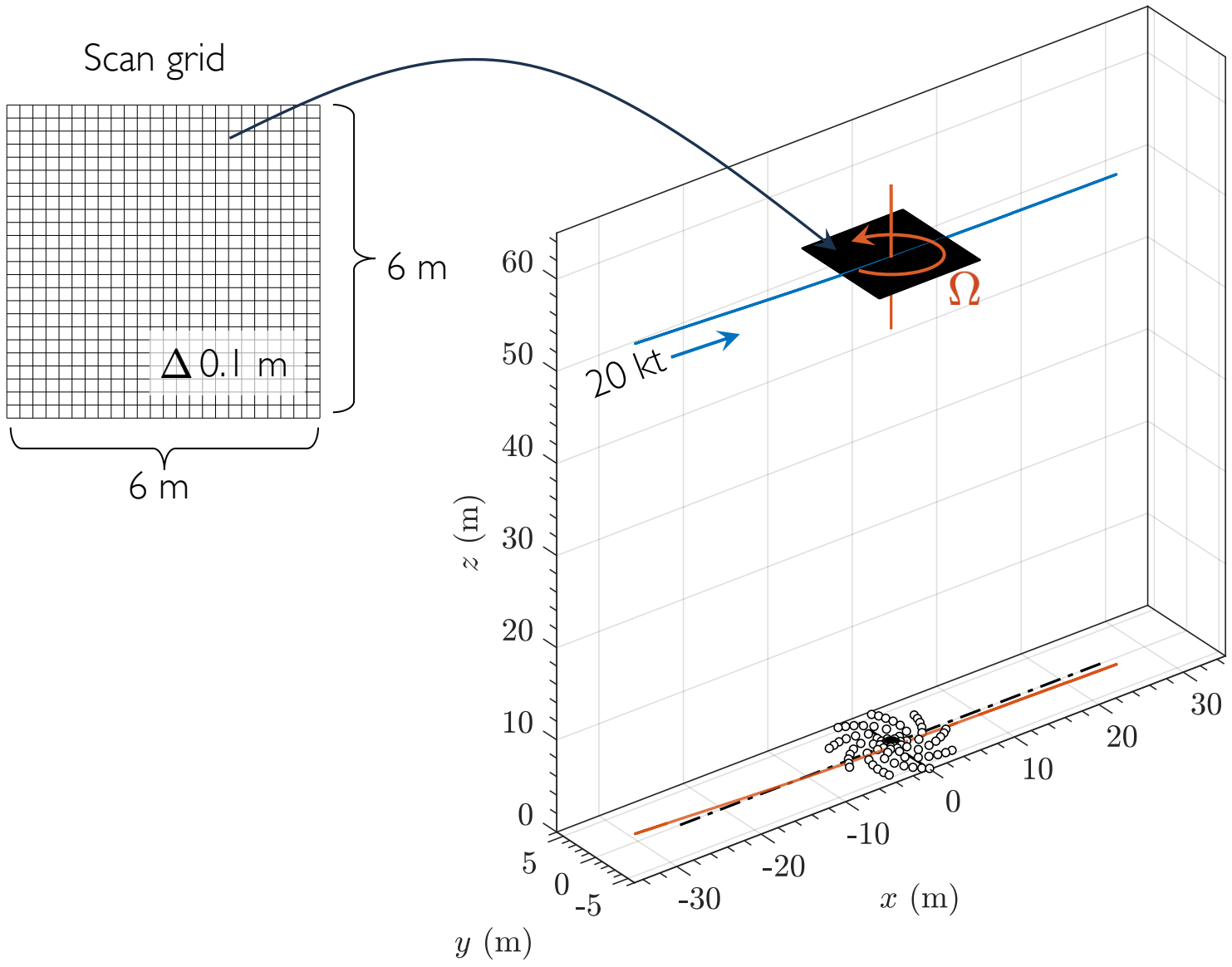

ROtating Source Identifier (ROSI)

- Scan grid translates to follow main rotor hub, and rotates at measured rotation rate, Ω
- Signals are transformed to source time (de-Dopplerization) for each grid point and microphone combination
  - 1.7 million pairs!

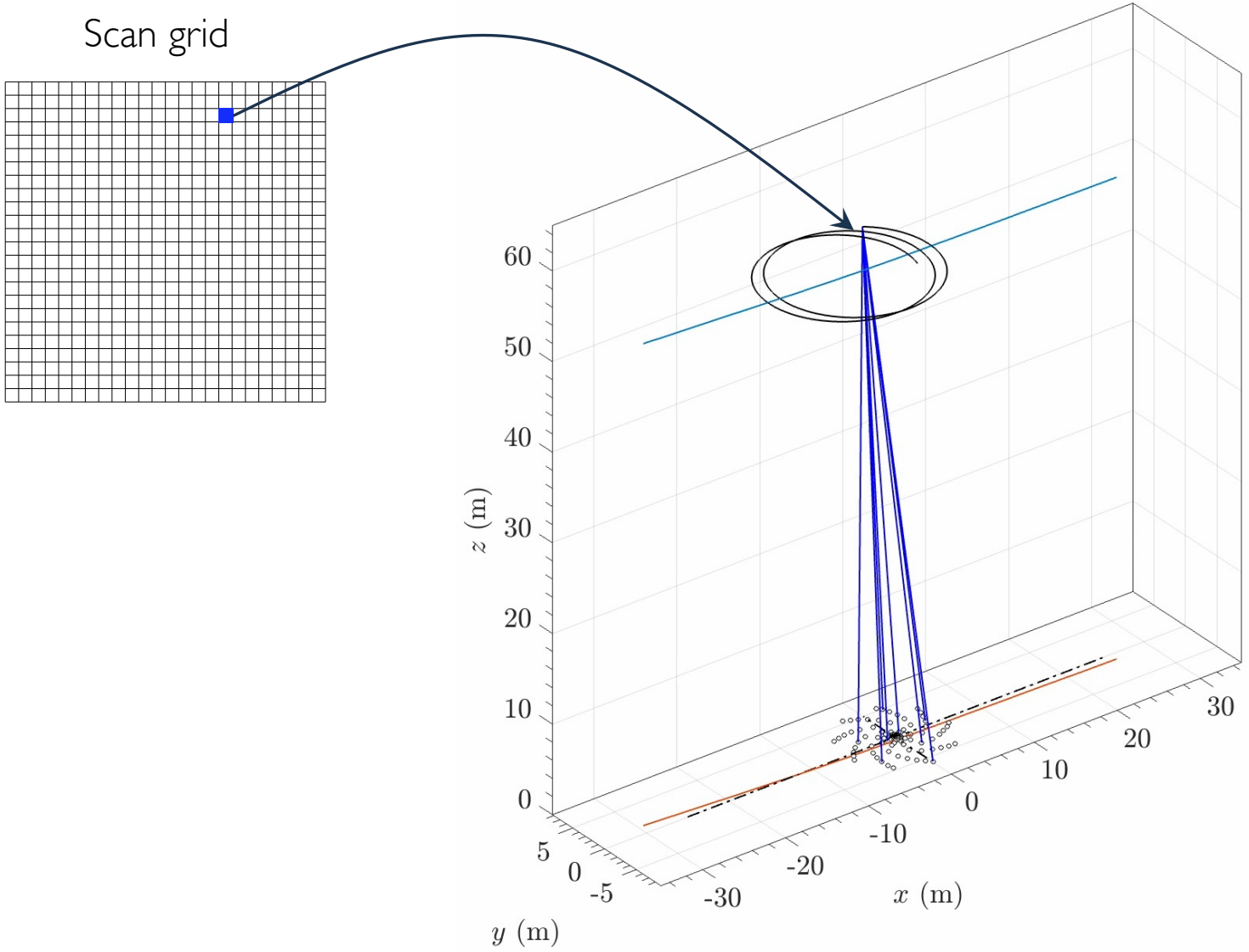

ROtating Source Identifier (ROSI)

- Scan grid translates to follow main rotor hub, and rotates at measured rotation rate, Ω

- Signals are transformed to source time (de-Dopplerization) for each grid point and microphone combination
  - 1.7 million pairs!

- Source strengths at each grid point are determined via a summation in the time,

$$\sigma_j(\tau) = \frac{1}{N}\sum_{n=1}^{N}\tilde{\sigma}_{j,n}(\tau)$$

or frequency domain,

$$A_{j,k} = \frac{1}{2N(N-1)}\sum_{n=1}^{N}\sum_{\substack{m=1\\m\neq n}}^{N}\mathcal{F}_k(\tilde{\sigma}_{j,n})\mathcal{F}_k(\tilde{\sigma}_{j,m})^*$$

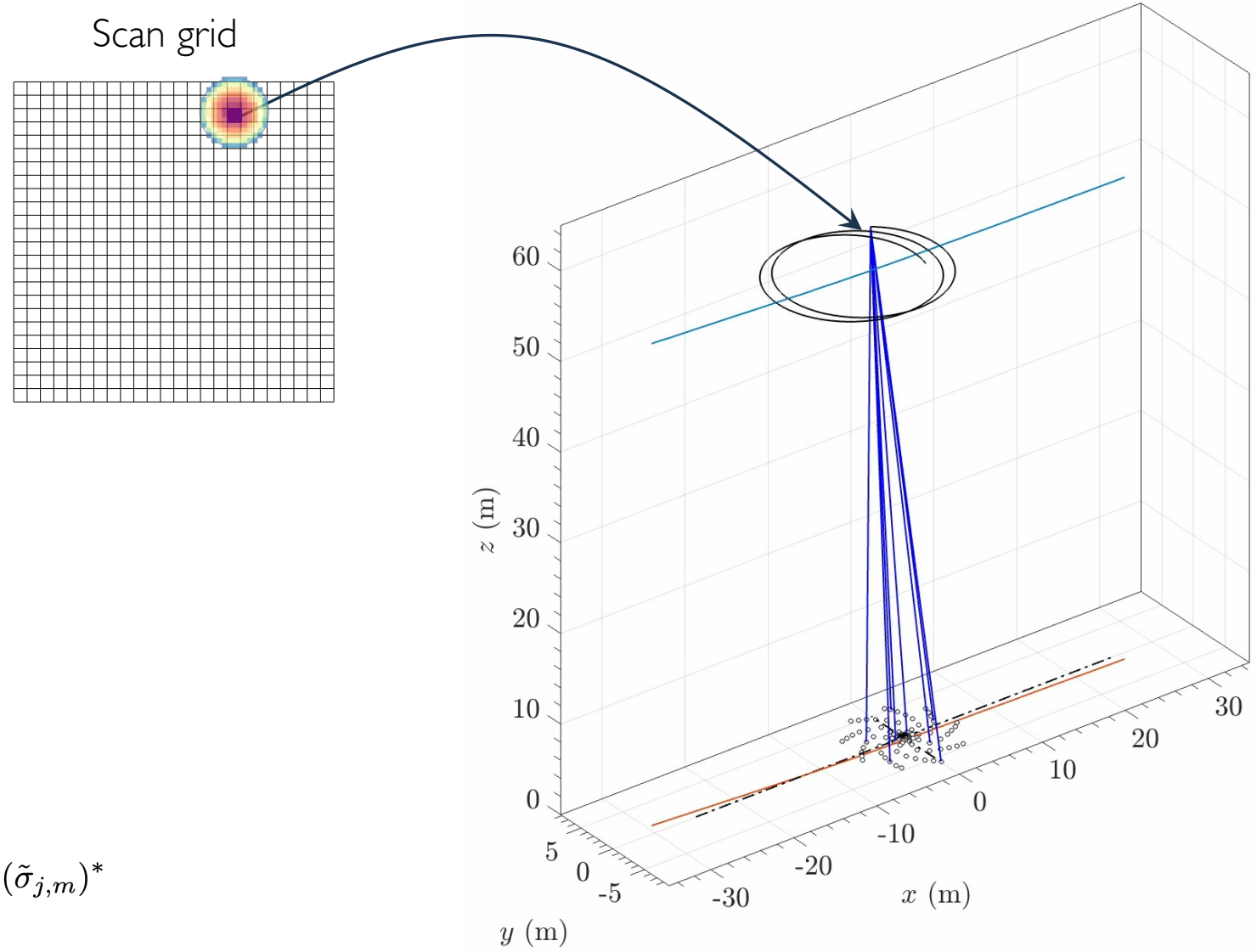

Effect of flight altitude

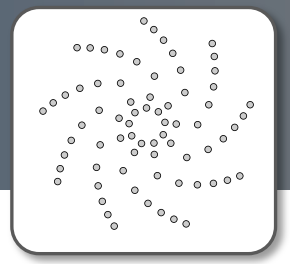

Outer array only
Uniform weighting

National Aeronautics and
Space Administration

Effect of flight altitude

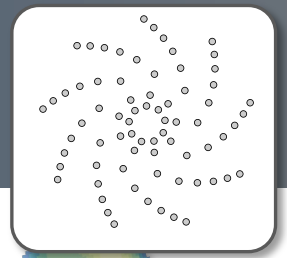

Outer array only
Uniform weighting

National Aeronautics and Space Administration

	500 Hz	1 kHz	2 kHz	4 kHz
60 m AGL	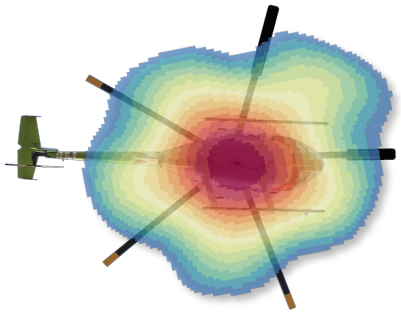	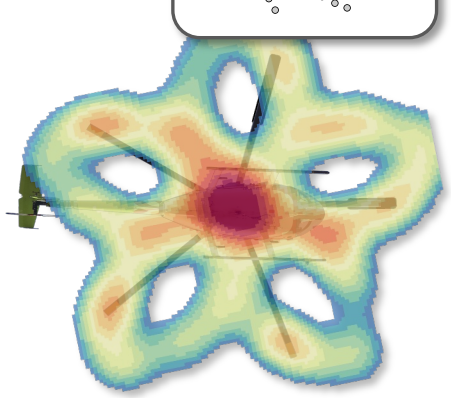	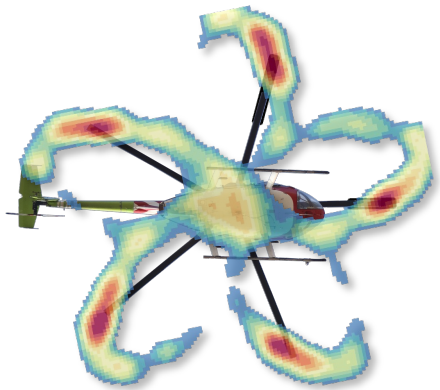	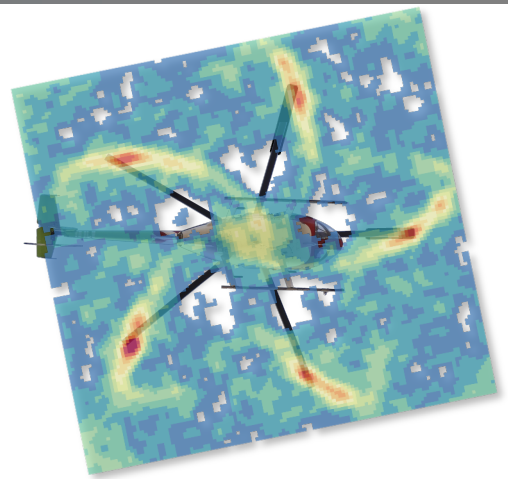

Effect of flight altitude

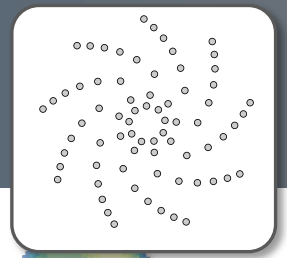

Outer array only
Uniform weighting

National Aeronautics and Space Administration

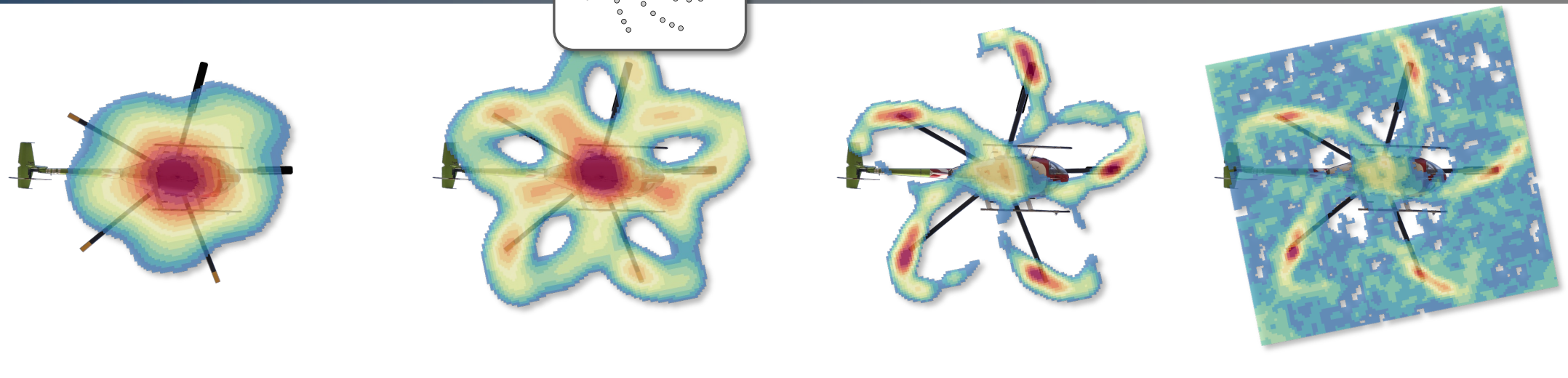

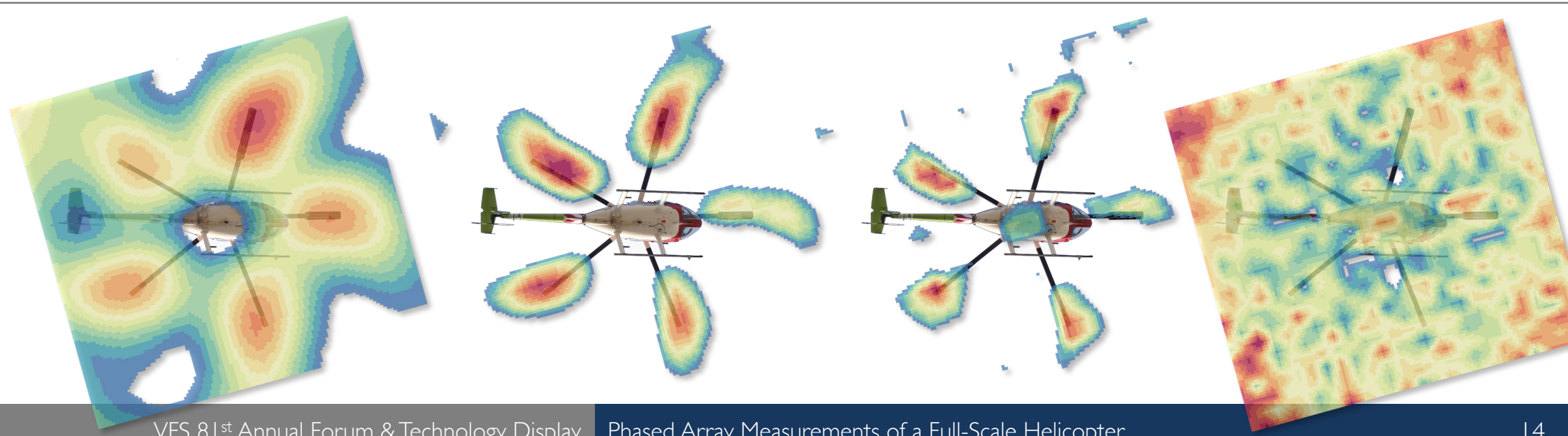

Array shading

No shading

$$A_{j,k} = \frac{1}{2N(N-1)} \sum_{n=1}^{N} \sum_{\substack{m=1 \\ m \neq n}}^{N} \mathcal{F}_k(\tilde{\sigma}_{j,n}) \mathcal{F}_k(\tilde{\sigma}_{j,m})^*$$

With shading

$$A_{j,k} = \frac{\sum_{n=1}^{N} \sum_{\substack{m=1 \\ m \neq n}}^{N} w_{k,n} w_{k,m} \mathcal{F}_k(\tilde{\sigma}_{j,n}) \mathcal{F}_k(\tilde{\sigma}_{j,m})^*}{2 \sum_{n=1}^{N} \sum_{\substack{m=1 \\ m \neq n}}^{N} w_{k,n} w_{k,m}}$$

Frequency-based weighting per microphone

Array shading

$$A_{j,k} = \frac{\sum_{n=1}^{N} \sum_{\substack{m=1 \\ m \neq n}}^{N} w_{k,n} w_{k,m} \mathcal{F}_k(\tilde{\sigma}_{j,n}) \mathcal{F}_k(\tilde{\sigma}_{j,m})^*}{2 \sum_{n=1}^{N} \sum_{\substack{m=1 \\ m \neq n}}^{N} w_{k,n} w_{k,m}}$$

- Weighting accounts for
  - Microphone density
    - Frequency independent; de-emphasizes central mics
  - Coherence over array
    - Frequency dependent; outer mics de-emphasized at high frequencies

500 Hz | 1 kHz | 2 kHz | 4 kHz

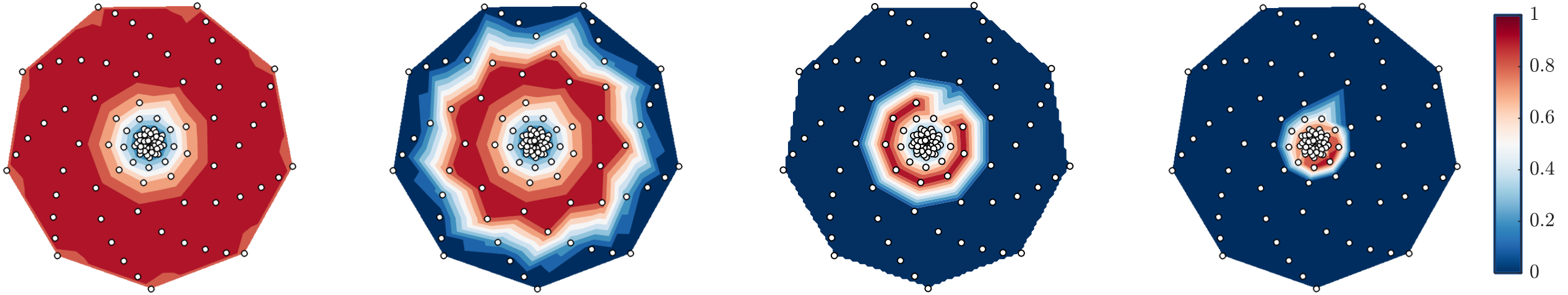

Coherence over array

- Gaussian-based curve fits of de-Dopplerized signals enable determination of length scale
- Frequency-dependent length scale approximately inversely proportional to frequency

200 Hz

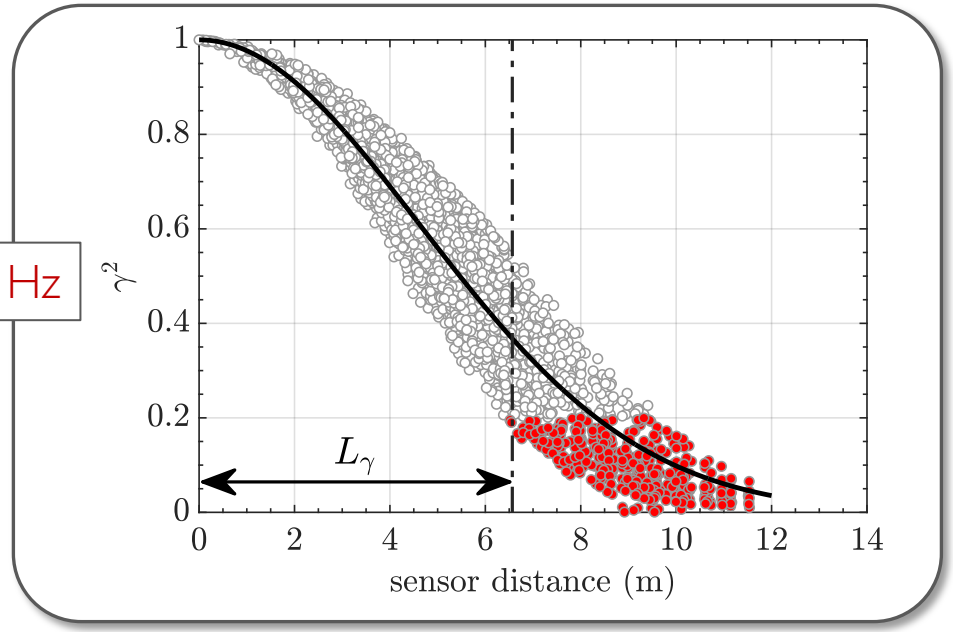

2 kHz

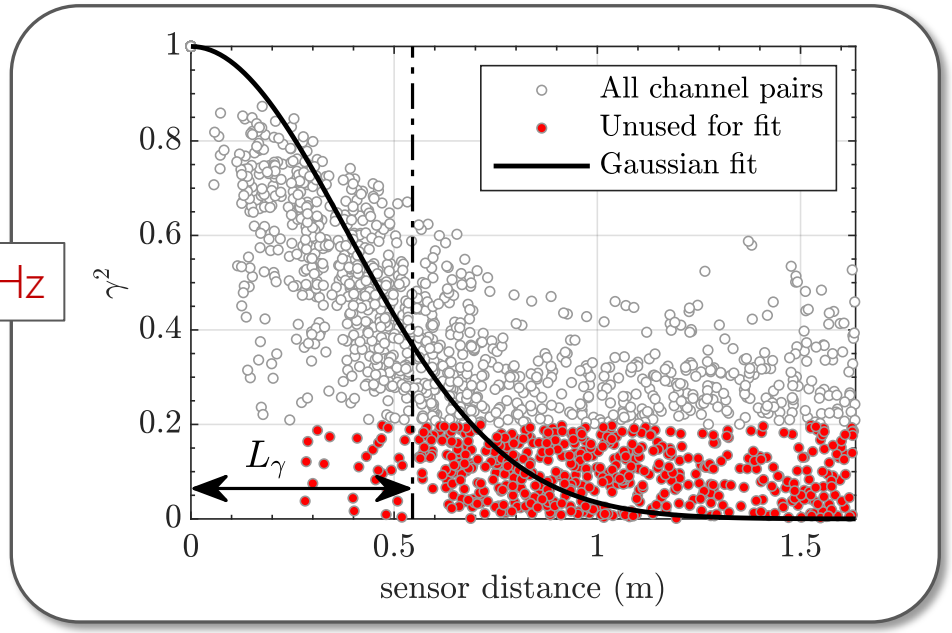

Coherence over array

- Gaussian-based curve fits of de-Dopplerized signals enable determination of length scale
- Frequency-dependent length scale approximately inversely proportional to frequency

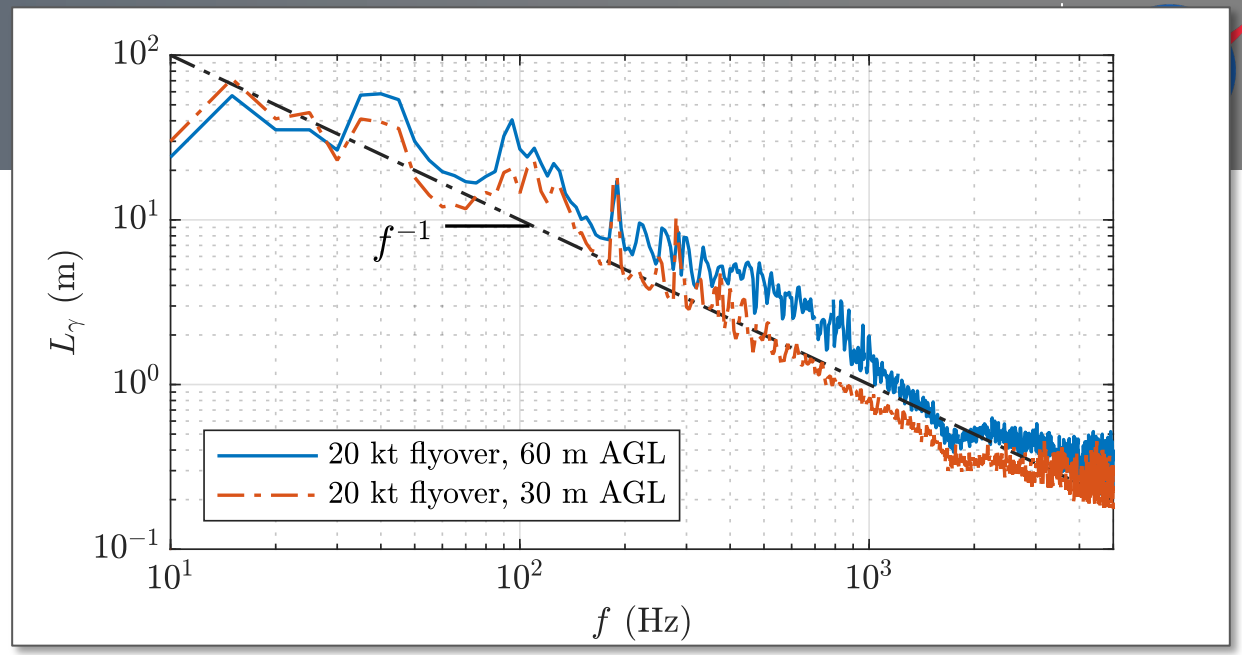

200 Hz

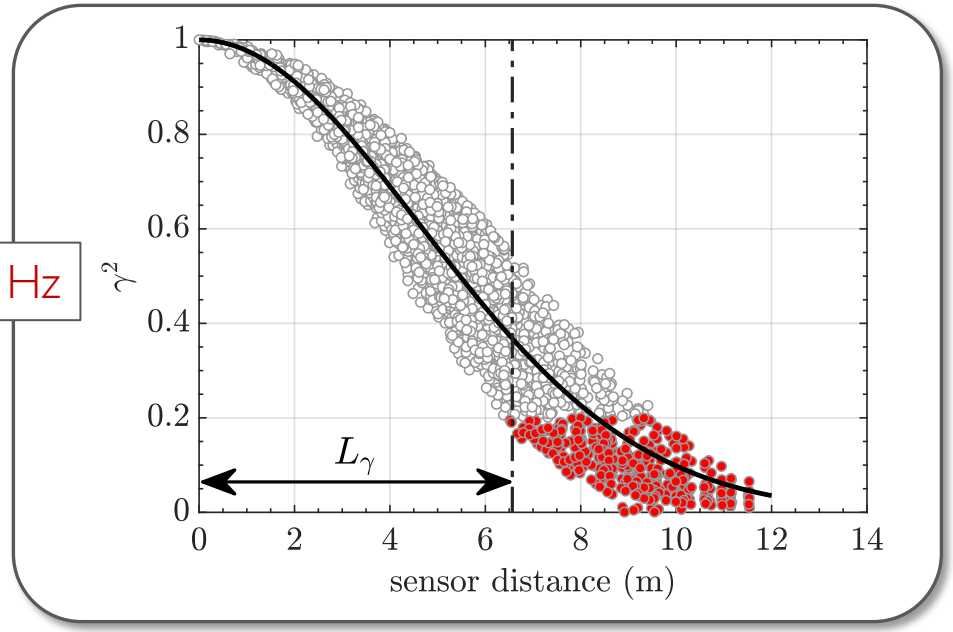

2 kHz

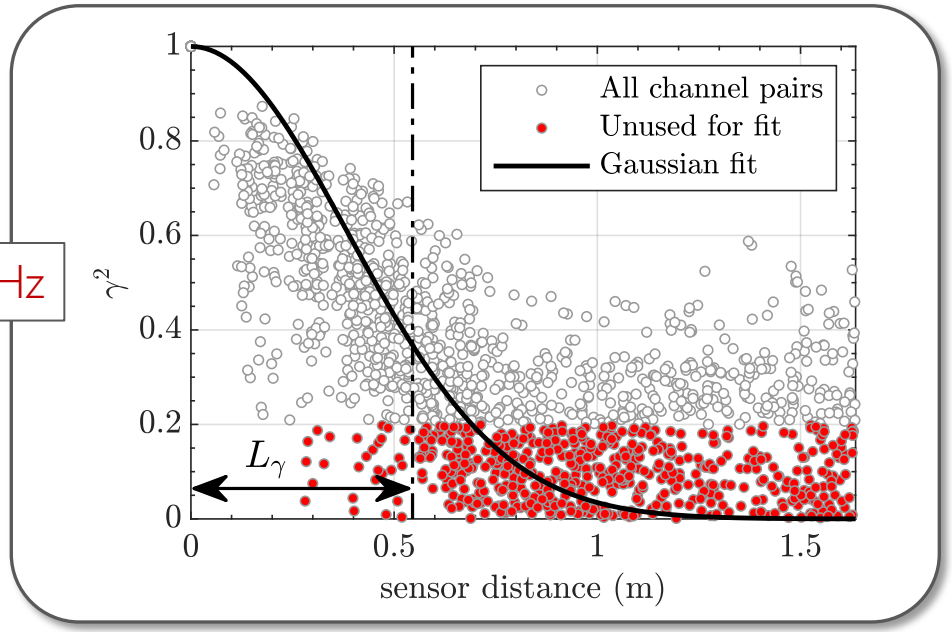

Improvement with shading

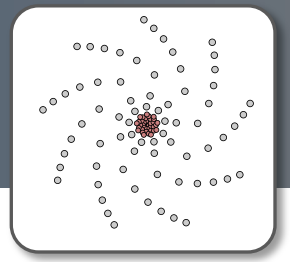

All mics (outer + inner)
Nonuniform weighting

- 30 m AGL, weighted scheme employed

500 Hz 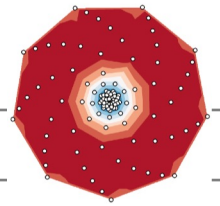

1 kHz 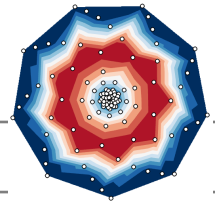

2 kHz 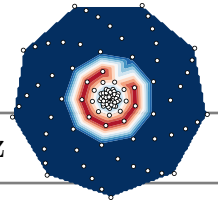

4 kHz 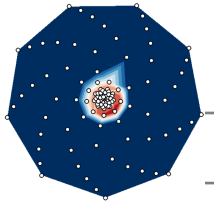

Improvement with shading

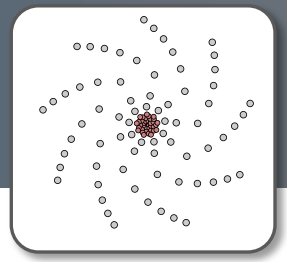

All mics (outer + inner)
Nonuniform weighting

National Aeronautics and Space Administration

- 30 m AGL, weighted scheme employed

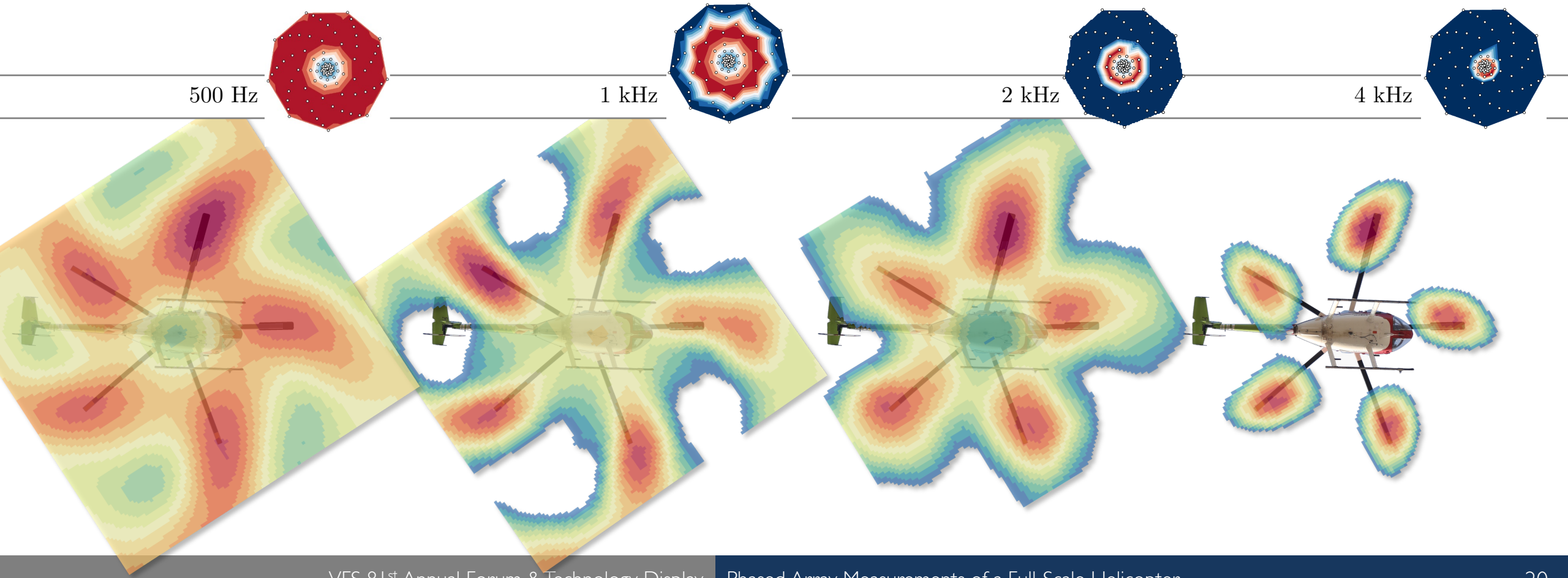

Improvement with shading

No shading

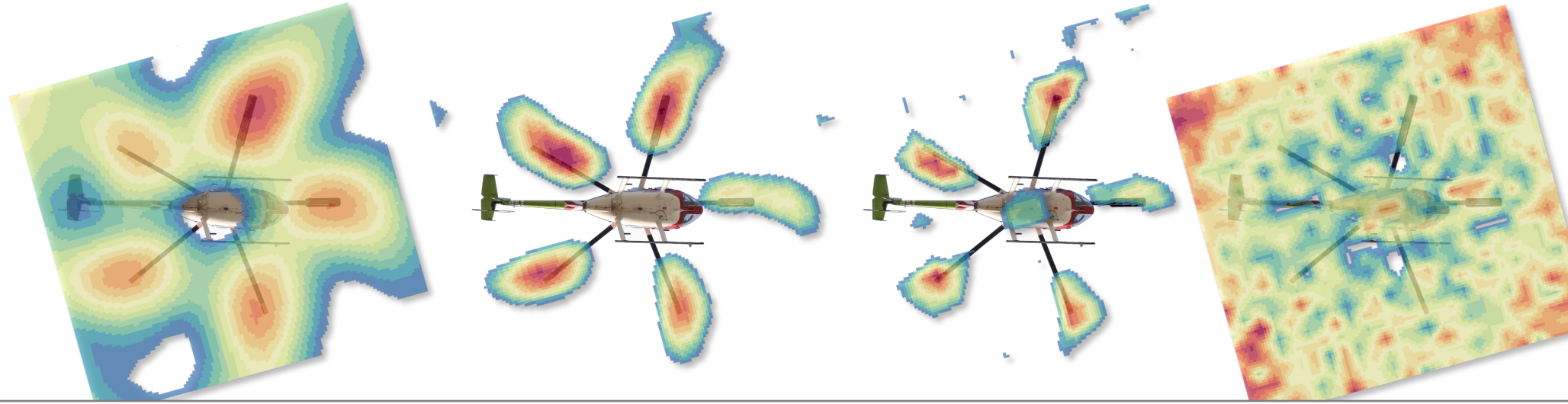

500 Hz | 1 kHz | 2 kHz | 4 kHz

With shading

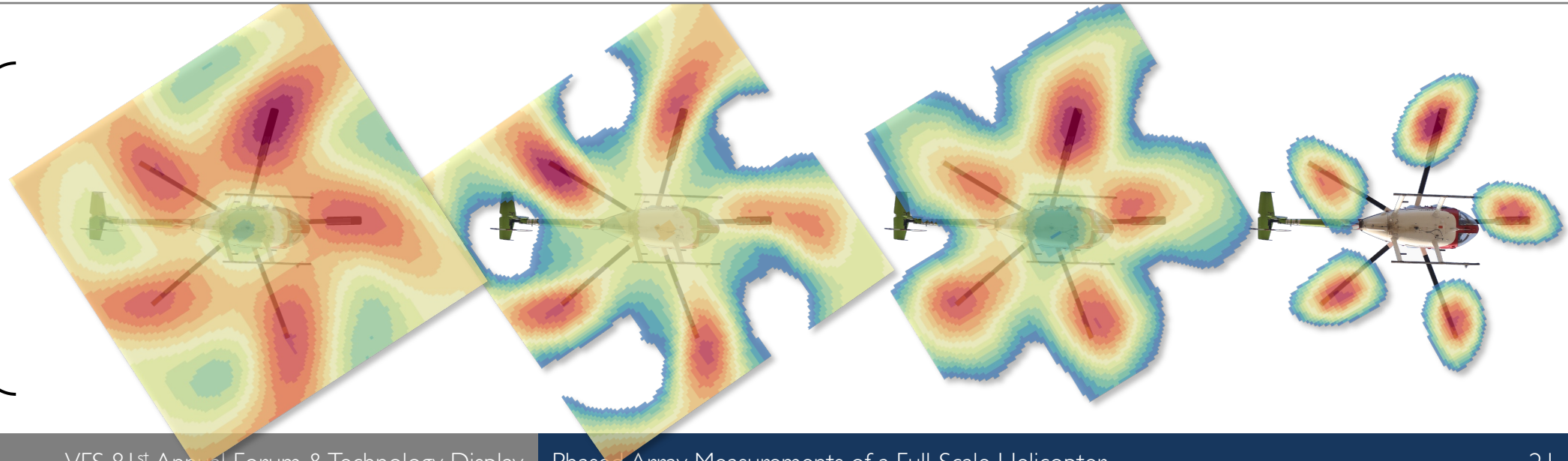

Integrated spectra

Integrate power over regions of the source maps → source ranking

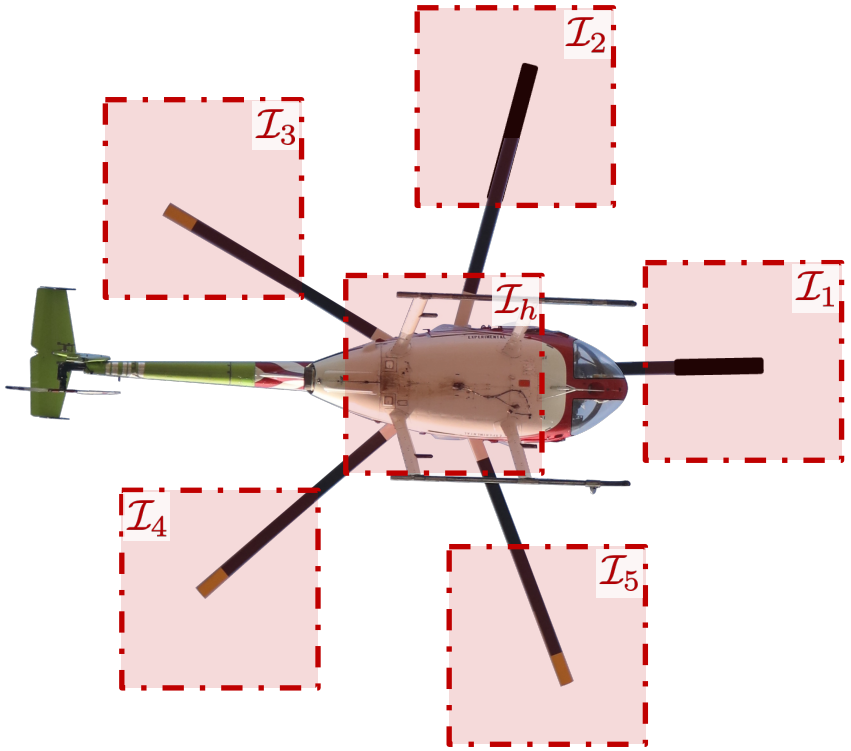

Integrated spectra

Integrate power over regions of the source maps → source ranking

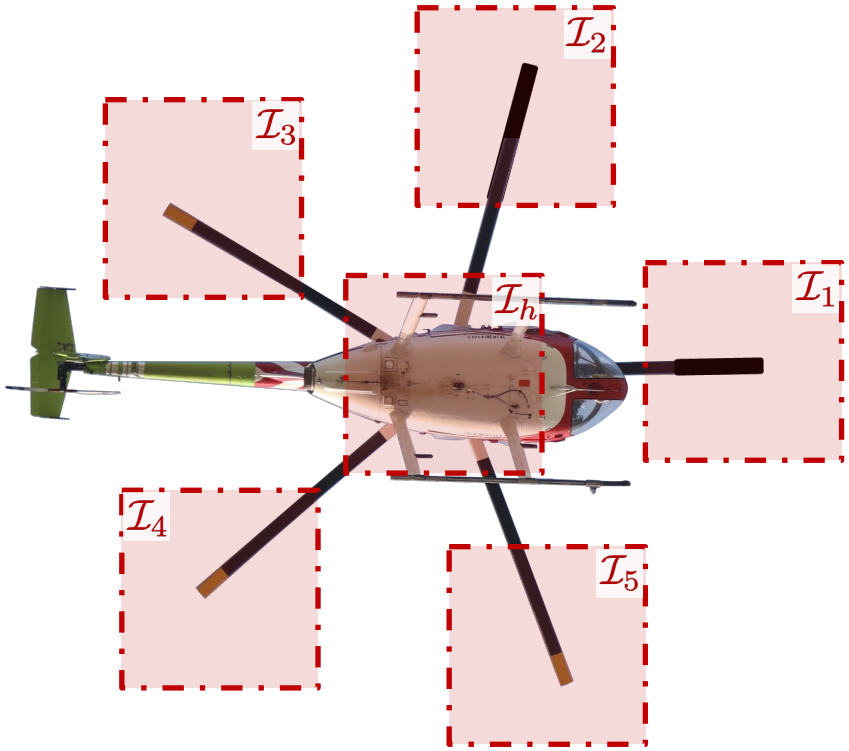

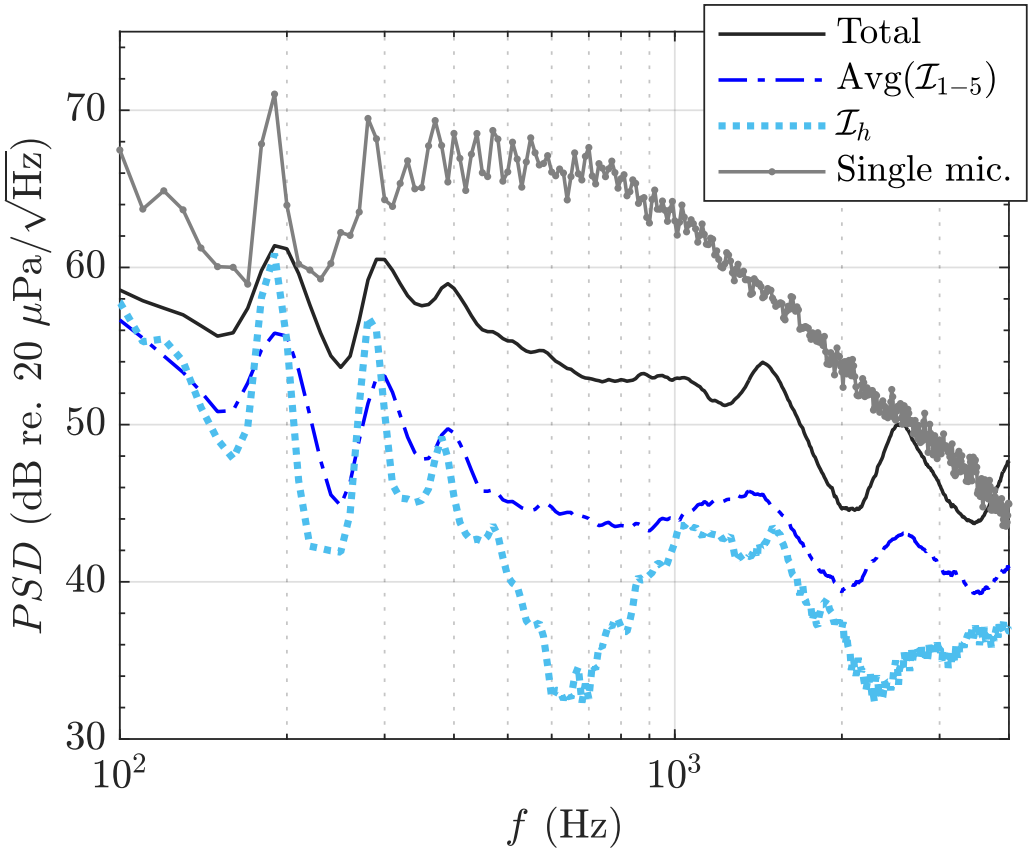

Average individual blade levels higher than noise found at hub

Integrated spectra

Integrate power over regions of the source maps → source ranking

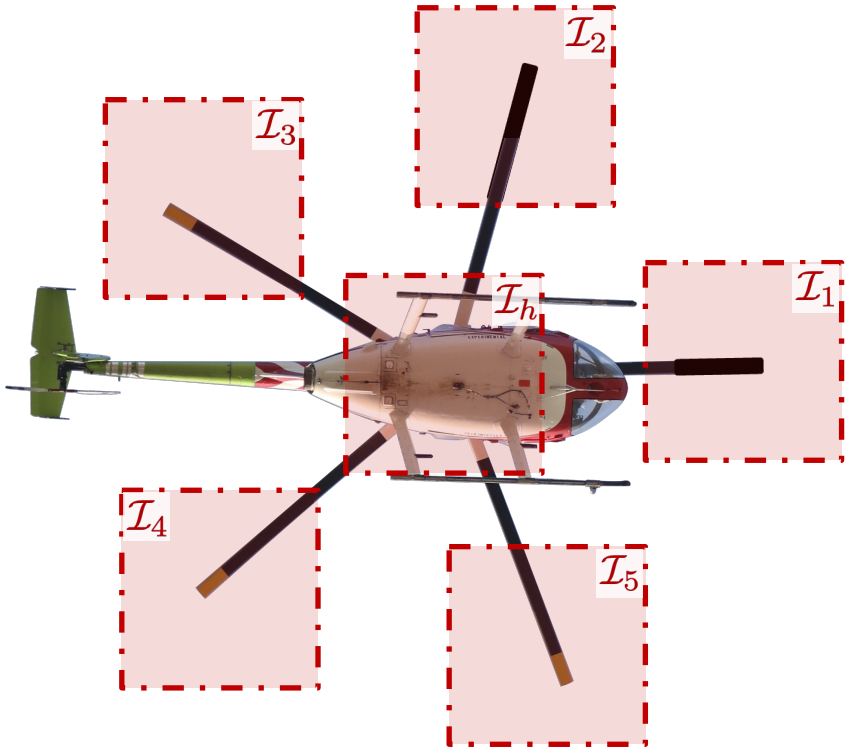

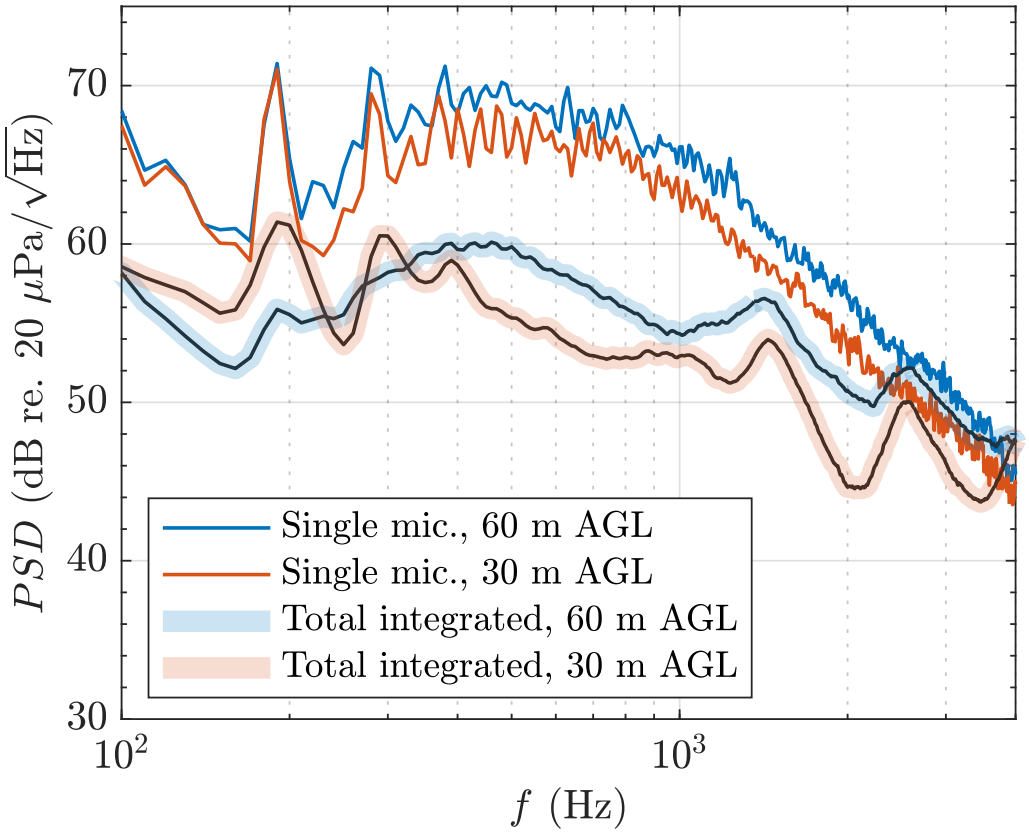

Reasonable consistency between two flights

Concluding remarks

- First attempt at applying rotating source beamforming to a helicopter in **forward flight**
- Initial results are promising, enabling isolation of nondeterministic noise of the main rotor
- What we learned:
  - Constraints on array aperture (size) – too big reduces coherence over array
  - Flight altitude should be carefully chosen relative to array size (spatial resolution effects)
  - Necessary to include shading schemes to visualize sources over broad frequency range
  - Coherence-based shading improved source maps at all frequencies
  - Limited number of rotor revolutions – may require multiple flyovers at higher flight speeds
- With appropriately designed array, method is suitable for UAM/FVL

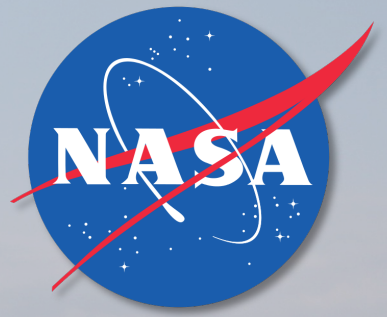

This work was supported by the the U.S. Army, Combat Capabilities Development Command Aviation & Missile Center, and the NASA Aeronautics Research Mission Directorate, Revolutionary Vertical Lift Technology Project.